Available online at www.sciencedirect.com
SCIENCE DIRECT
Thermochimica Acta 445 (2006) 151–159
thermochimica acta
www.elsevier.com/locate/tca

Calorimeters for biotechnology

Donald J. Russell [a,*], Lee D. Hansen [a,b]

[a] *Calorimetry Sciences Corp., 890W 410N, Suite A, Lindon, UT 84042 USA*
[b] *Department of Chemistry and Biochemistry, Brigham Young University, Provo, UT 84602 USA*

Abstract

The isothermal and temperature scanning calorimeters manufactured by Calorimetry Sciences Corporation are briefly described. Applications of calorimetry to determine thermodynamics and kinetics of reactions of interest in biotechnology are described with illustrative examples.

Keywords: Calorimetry; Proteins; Lipids; Membranes; Equilibrium constant; Transitiometry; Pressure-perturbation; DSC; ITC

1. Introduction

Calorimetry plays an important role in biotechnology. Determination of the kinetics and thermodynamics of reactions of biological molecules is necessary for understanding the structures and functions of these molecules, and in bioengineering living systems (e.g. see [1–6]), and for making pharmaceutical preparations (e.g. see [7–9]). This paper first gives a brief review of the calorimeters manufactured by Calorimetry Sciences Corporation (CSC), then describes some applications of differential temperature scanning calorimetry (DSC) and of isothermal calorimetry in biotechnology.

2. Calorimeters manufactured by CSC

Table 1 lists the six standard calorimeters produced and their characteristics. All of these calorimeters can be used to measure thermodynamics and kinetics of reactions of biological systems. The calorimeters cover a range of sample sizes from 0.3 to 150 mL (a few micrograms to hundreds of grams of sample) and a range of detection limits on heat rate measurement from microwatts to nanowatts. CSC also manufactures several other specialized calorimeters and adaptations of the standard calorimeters discussed here.

The model 4400 IMC is a heat conduction calorimeter with a detection limit <1 μW that accommodates samples up to 150 mL in volume. This calorimeter is particularly useful for determination of kinetics of slow reactions where the amount of material is not limiting (e.g. see [9–13]). The model 4500 INC is a heat conduction calorimeter with a detection limit of <40 nW. This calorimeter is particularly useful for determination of kinetics of slow reactions, heats of solution of solids, and incremental titrations for simultaneous determination of equilibrium constants and enthalpy changes with limited amounts of material (e.g. see [2,9,14,15]). The model 4300 ISC is an isoperibol, temperature-rise, solution calorimeter [16,17]. The reaction vessels for this calorimeter are special glass Dewars with equilibration times of <1 s [18]. This feature makes this calorimeter particularly useful for determination of kinetics of reactions that are too fast to study easily by heat conduction calorimetry. The rapid equilibration allows rapid, continuous titrations, which makes it possible to obtain data much faster with this calorimeter than with heat conduction calorimeters [16,19]. A titration curve with 50–100 data points only requires about 1 h for the entire operation, including the initial equilibration. Obtaining many, closely spaced, data points provides a significant advantage in determination of equilibrium constants [20–23]. The model 4100 MC-DSC is a heat conduction, temperature scanning calorimeter with three sample cells and one common reference cell. Removable ampules make it easy to sterilize and load the sample ampules. Sample sizes from a few microliters (or mg) up to 1 mL (or 1–2 g) can be used in this calorimeter. This calorimeter can also be operated in an isothermal mode to determine isothermal kinetics of slow reactions (e.g. see [24–27]. The mod-

* Corresponding author. Tel.: +1 801 763 1500; fax: +1 801 763 1414.
E-mail addresses: rusty.russell@calscorp.com (D.J. Russell), lee_hansen@byu.edu (L.D. Hansen).

0040-6031/$ – see front matter © 2005 Elsevier B.V. All rights reserved.
doi:10.1016/j.tca.2005.08.023

Table 1
Calorimeters manufactured by Calorimetry Sciences Corporation

Specifications		Measurements
IMC Model 4400—isothermal heat conduction calorimeter		
Sample size	Up to 150 mL removable, solid or liquid	Incremental titration, sealed ampule, liquid flow sorption, batch (solid or liquid), gas sorption, flow mixing, water vapor sorption, high pressure
Temperature range (°C)	−40 to 80, 0–100, 0–200	
Detectable heat effect (μJ)	40	
Baseline stability (μW)	1	
Noise level (μW)	±0.1	
INC Model 4500—isothermal heat conduction calorimeter		
Sample size	Up to 2 mL removable, solid or liquid	Incremental titration, gas sorption, liquid flow sorption, batch (solid or liquid), water vapor sorption, sealed ampule, high pressure
Temperature range (°C)	0–110	
Detectable heat effect (μJ)	0.4	
Baseline stability (nW)	40	
Noise level (nW)	±4	
ISC Model 4300—isoperibol temperature-rise calorimeter		
Sample size	25 or 50 mL Dewar, liquid	Continuous titration, incremental titration, batch (solid or liquid)
Temperature range (°C)	0–100	
Detectable heat effect (mJ)	4	
Temperature stability	100 μ°C/24 h	
Temperature noise (μ°C)	±30	
MC-DSC Model 4100—scanning and isothermal heat conduction calorimeter		
Sample size	Up to 1 mL removable, solid or liquid	Batch (solid or liquid), sealed ampule, water vapor sorption, gas sorption, high pressure
Temperature range	−40 to 110 °C, −40 to 200 °C	
Baseline stability (μW)	2	
Noise level (μW)	±0.2	
Scan rates	Up to 2 °C/min	
Model 5300 Nano-ITC III—isothermal power compensation calorimeter		
Sample size	1 mL fixed in place, liquid	Incremental titration, continuous heat rate
Temperature range (°C)	2–80	
Detectable heat effect (μJ)	0.1	
Baseline stability (nW)	80	
Noise level (nW)	±4	
Model 6100/6300 Nano-DSC II/III—scanning and isothermal power compensation calorimeter		
Sample size	0.3 mL fixed in place, capillary or cylindrical	Temperature scanning (pressure perturbation model 6300 only)
Temperature range (°C)	−10 to 130, −10 to 160	
Scan rates	Up to 2 °C/min	
Baseline stability (nW)	28	
Noise level (nW)	±15	

els 6100/6300 DSC-II/III are power compensation, temperature scanning calorimeters with a heat rate detection limit of 15 nW. The DSC-II/III is available with either cylindrical or capillary cells, both with cell volumes of 0.3 mL of a liquid sample. A pressure perturbation accessory is built into the DSC-III. Pressure is generated by a programmable syringe that can be driven at various rates to accommodate systems that equilibrate slowly. The model 5300 ITC-III is an isothermal power compensation calorimeter with a motor-driven syringe and a variable speed stirrer for incremental titrations. The ITC-III has a heat rate detection limit of 4 nW in unstirred solutions. The detection limit in stirred solutions depends on the stirring rate and sample properties.

3. Examples of applications of differential temperature scanning calorimetry to biotechnology

DSC can be used to study thermally induced conformational changes in biopolymers and lipid membranes and ligand and binding to biopolymers and biomembranes (e.g. see [3,5]). Changes in heat capacity, enthalpy, and entropy accompanying changes in conformation or binding are commonly determined. Free energies, compressibilities, and thermal expansion coefficients can also be determined by combining calorimetry with pressure–volume changes, a method called transitiometry in the physical chemistry literature (e.g. see [28–33]) and pressure perturbation in the polymer and biotechnology literature (e.g. see [34,35]).

The initial data collected from a DSC temperature scan are in microwatts (or $\mu J\,s^{-1}$). An example of typical raw data for protein denaturation is shown in Fig. 1. This figure illustrates both the small amount of protein required and the baseline reproducibility available with current instruments. Integration of the raw data peak in time gives the calorimetric enthalpy change for the reaction. Alternately, raw data can be converted to heat capacity by dividing the heat rate by the scan rate, i.e. $C = \phi\ (\mu J\,s^{-1})/\beta\ (K\,s^{-1})$, and integration of the heat capacity peak over temperature gives the calorimetric enthalpy change. Note

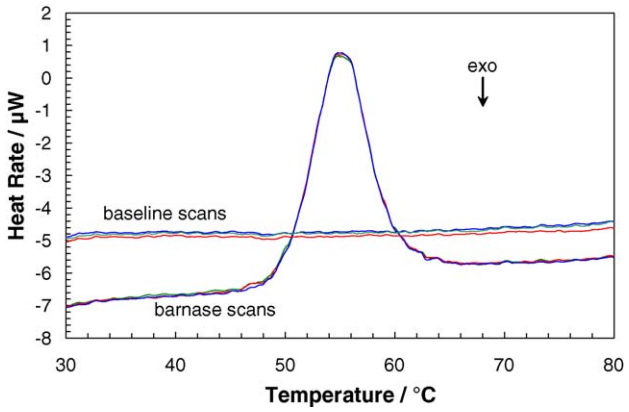

Fig. 1. Three baseline temperature scans and three temperature scans of 60 μg of barnase protein in 0.3 mL of solution in a CSC model 6100 DSC-II. (Data courtesy of Peter Privalov, Johns Hopkins University.)

that the scan rate is not necessarily a constant. Fig. 2 shows an example of data plotted as heat capacity versus temperature for a solution of lysozyme at conditions commonly used as a test system. Note the shift in the baseline between 50 and 80 °C that indicates a change in the heat capacity between the native and denatured states. Partial molar heat capacities of the native and denatured lysozyme and their temperature dependencies can be read directly from the plot.

Fig. 3 shows data for uncoiling of the domains in double-stranded DNA together with optical data on the same sample. Note the general agreement between the two methods. Deconvolution and integration of the peaks gives the total enthalpy change for uncoiling of each domain. Division by the average enthalpy change per base pair gives an estimate of the number of base pairs in each domain. Fig. 4 shows determinations of the enthalpy change per base pair with binding of oligomers of poly-rA to poly-rU. Concentrations down to about 50 μM gave results precise to <0.5%. Note that the calorimetric data extend down to the same concentrations as the optical method.

Fig. 5 shows the transitions observed in vesicles of DPPC. The pre-transition at about 35 °C and the main gel to liquid–crystal transition are readily apparent. Vesicle structure (e.g. monolamellar versus multilamellar, pure DPPC versus mixtures with other lipids, ion binding to the surface) greatly affects the data obtained from such scans, and thus DSC is a sensitive method for studying the structures of lipid membranes.

Fig. 6 shows the effect of Ca^{2+} binding on unfolding of rat parvalbumin. The peaks can be integrated to obtain the enthalpy change for the transition in each case. The difference in the enthalpy changes is an estimate of the enthalpy of binding of Ca^{2+} ions to the native protein.

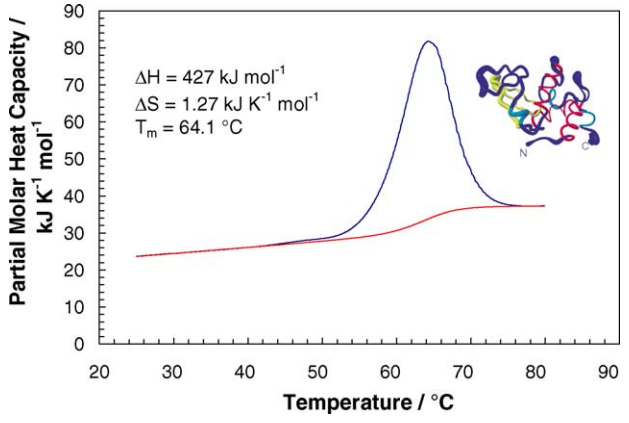

Fig. 2. Temperature scan, converted to heat capacity, and fitted baseline for 1 mg mL^{-1} lysozyme solution in a CSC model 6100 DSC-II.

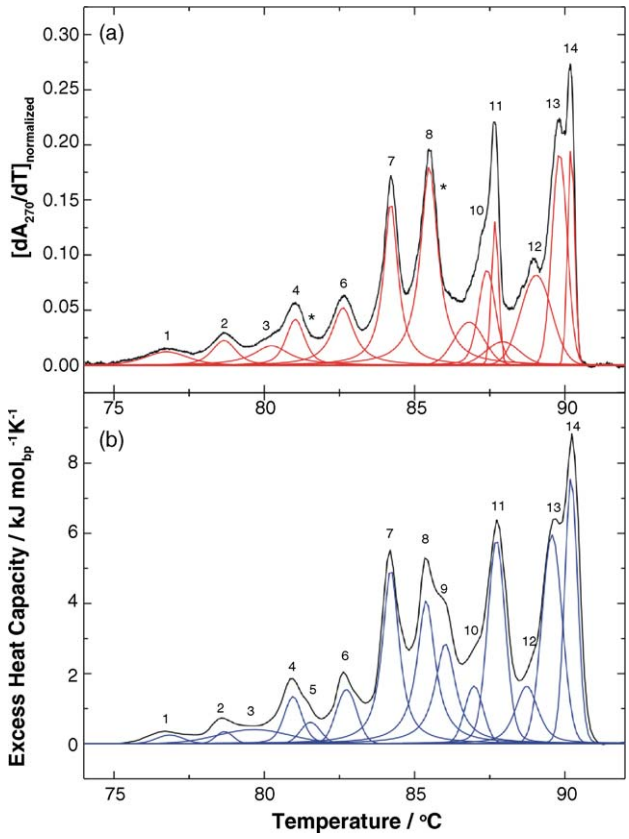

Fig. 3. Optical scan compared with a thermal temperature scan of double-stranded DNA in a CSC model 6100 DSC-II. (Data courtesy of Jens Völker and Kenneth J. Breslauer, Rutgers University.)

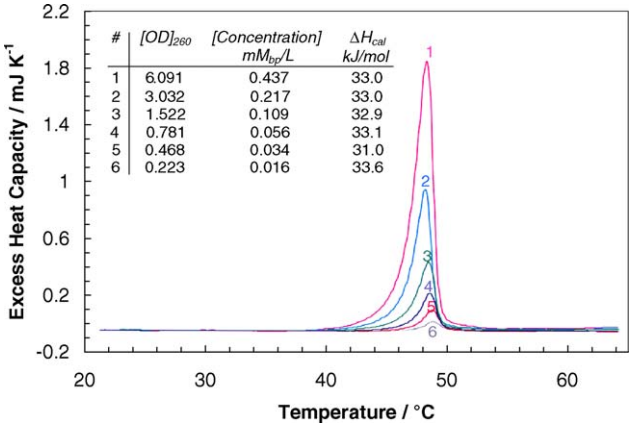

#	[OD]260	[Concentration] mMbp/L	ΔHcal kJ/mol
1	6.091	0.437	33.0
2	3.032	0.217	33.0
3	1.522	0.109	32.9
4	0.781	0.056	33.1
5	0.468	0.034	31.0
6	0.223	0.016	33.6

Fig. 4. Temperature scans of poly-rA/poly-rU oligomers as a function of concentration in a CSC model 6100 DSC-II. (Data courtesy of Jens Völker and Kenneth J. Breslauer, Rutgers University.)

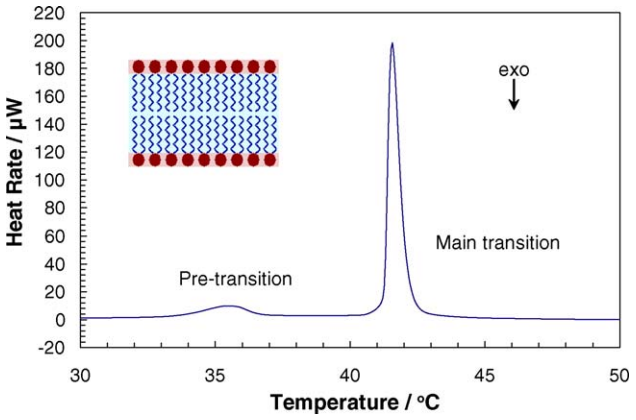

Fig. 5. Temperature scan of DPPC vesicles in a CSC model 6300 DSC-III.

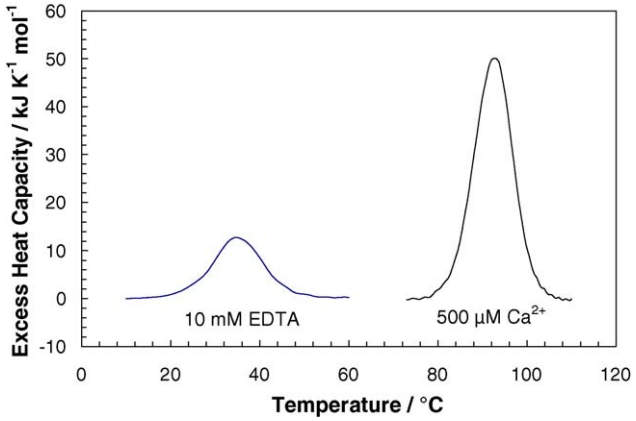

Fig. 6. Temperature scans of rat parvalbumin in the presence of 10 mM EDTA and of 0.5 mM Ca^{2+} in a CSC model 6100 DSC-II. (Data courtesy of Michael T. Henzl, University of Missouri, Columbia.)

The thermally induced transitions in organelles in whole cells can be seen in temperature scans of the cells as shown in Fig. 7 [36]. Such data can be used to determine the effects of various contaminants and preservatives on the stabilities of the structures in the organelles.

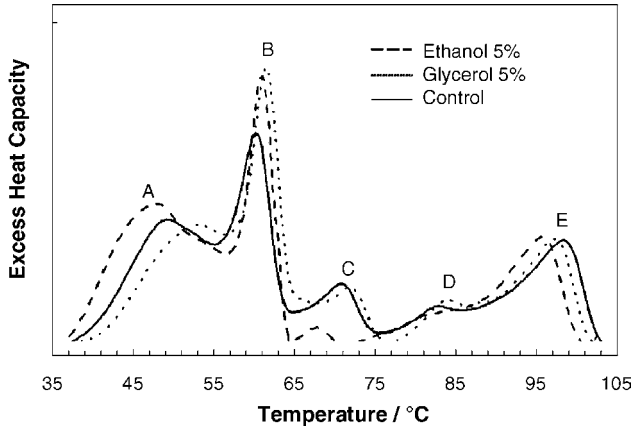

Fig. 7. Temperature scans of Chinese hamster lung V79 cells in various media. (Reproduced by permission from [36].)

4. Examples of applications of isothermal calorimetry to biotechnology

Isothermal titration calorimetry can be used to study the intermolecular interactions of both small and large molecules (e.g. see [2]). Enthalpy changes, and under some conditions, free energy and entropy changes [2,14,15,20–23,37,38], can be determined by titration calorimetry. Titration calorimetry can also be used to determine enthalpy changes for conformational changes in biopolymers and membranes that are induced by changes in composition of the solvent. Isothermal batch calorimetry is used to determine heats of reactions where the reaction goes to completion and the amount of reaction is limited by one reagent, e.g. heats of solution of solids. Isothermal calorimetry can also be used to determine the kinetics of reactions such as enzyme catalyzed reactions and of metabolism of cell cultures, tissues and whole organisms [1,4,5].

Determination of equilibrium constants by calorimetry has been done for many years [39]. The method was fully developed shortly after accurate, continuous titration, temperature-rise calorimeters became available [14,18,20–22,37,38]. Early work with this method was mostly done on systems where relatively large amounts of reactants were available. When small volume heat conduction calorimeters that required much less material became available, the method was adapted for determination of equilibrium constants for ligand binding to biomolecules such as proteins and cell receptors [15].

Typical data for titration of a solution of ligand into a protein are shown in Fig. 8. Each peak in Fig. 8a represents the heat produced by addition of a fixed volume of titrant solution into the protein solution. Integration of the peaks over time results in the data shown in Fig. 8b where the number of microjoules in each peak is plotted against the mole ratio of titrant to titrate. The horizontal axis can also be plotted as volume or moles of titrant added. Summing the heat from each injection and plotting the sums against the volume of titrant produces titration curves in the form commonly used to display data from continuous titration curves obtained with isoperibol temperature-rise calorimeters such as the CSC model 4300 ISC (e.g. see [14,16,18,19–22]. Either type of plot can be used to obtain equilibrium constants for incomplete reactions. Titration curves such as shown in Fig. 8b are typically used with data from incremental titrations done in heat conduction calorimeters and plots of total heat are used with data from continuous titrations done with temperature-rise calorimeters. This choice is a consequence of the uncertainty in the volume of titrant injected in the first injection in incremental titrations, and other experimental errors such as bubbles from inadequate degassing of solutions. These errors are not significant in properly conducted continuous titrations with larger volumes such as those used with the 4300 ISC.

Fig. 9 shows the effects of relative magnitudes of the enthalpy change (ΔH) and the equilibrium constant (K) for a 1:1 reaction on the shape of the titration curve. The curve obtained also depends on the concentrations of the reactants. Therefore, the lower the concentration, the larger the association constant that can be determined. Obtaining a useable titration curve for determining the equilibrium constant requires the product of

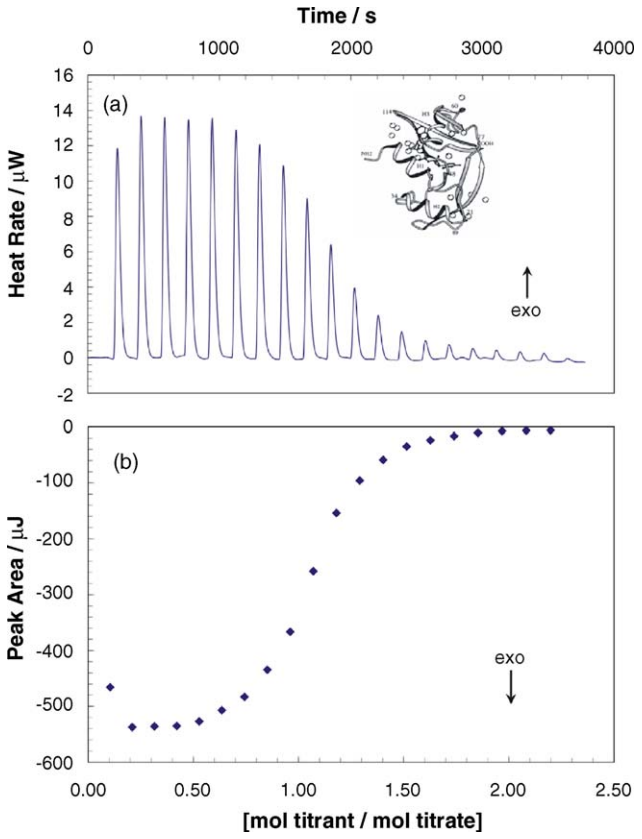

Fig. 8. RNAaseA titrated with 2′-CMP in a CSC model 5300 ITC-III. Part (a) shows the raw data. Part (b) shows the data after integration of each of the peaks from each injection.

the titrate concentration in moles per liter and the association constant to be between 10 and 1000. The calorimetric method for simultaneous determination of K and ΔH obviously is only applicable to reactions that are incomplete, but produce sufficient heat for accurate measurements.

To understand the basis of this method, consider a reaction described by

$$T\,(\mathrm{aq}) + R\,(\mathrm{aq}) = TR\,(\mathrm{aq}) \tag{1}$$

where T is the titrant and R is the reactant. The equilibrium constant expression for dissociation of TR is then

$$K = \frac{a_T a_R}{a_{TR}} = \left\{\frac{[T][R]}{[TR]}\right\}\left\{\frac{\gamma_T \gamma_R}{\gamma_{TR}}\right\} \tag{2}$$

where a is the activity, γ is the activity coefficient, and the brackets indicate molar concentration, i.e. moles/liter. Activity coefficients can be calculated from an extended Debye–Hückel equation or similar model if necessary. The total heat produced to any point in the titration is related to the enthalpy change for the reaction, ΔH, by

$$Q_i = (n_{TR})_i\,\Delta H = V_i[TR]_i\,\Delta H \tag{3}$$

where $(n_{TR})_i$ is the number of moles of TR at point i, V_i the total volume in the reaction vessel at point i, and $[TR]_i$ is the concentration of TR at point i. The mass balance equations for T and R at point i are

$$[T_{\mathrm{tot}}]_i = [T]_i + [TR]_i \tag{4}$$

and

$$[R_{\mathrm{tot}}]_i = [R]_i + [TR]_i \tag{5}$$

Combining the above four equations gives

$$K' = \left([T_{\mathrm{tot}}]_i - \frac{Q_i}{V_i\,\Delta H}\right)\frac{[R_{\mathrm{tot}}]_i - Q_i/V_i\,\Delta H}{Q_i/V_i\,\Delta H} \tag{6}$$

where

$$K' = \frac{K}{\gamma_T\gamma_R/\gamma_{TR}} \tag{7}$$

Rearranging gives

$$0 = \left(\frac{[T_{\mathrm{tot}}]_i[R_{\mathrm{tot}}]_i V_i}{Q_i}\right)(\Delta H)^2 + (-[T_{\mathrm{tot}}]_i - [R_{\mathrm{tot}}]_i - K')\,\Delta H + \frac{Q_i}{V_i} \tag{8}$$

which can be fit to the data by regression to evaluate K' and ΔH, or values for K' and ΔH can be obtained by successive approximation [40]. These equations are easily modified so they can be fit to incremental titration curves such as that shown in Fig. 8b.

Fig. 10a and b are included to show how different values of K and ΔH affect the fit to the data. These curves make it clear that the accuracy with which ΔH is determined depends primarily on the accuracy of the heat measured in the early part of the titration where the reaction is most nearly complete. The accuracy with which K can be determined depends on the number and accuracy of the data points in the more curved portion of the titration near the equivalence point. A common error made

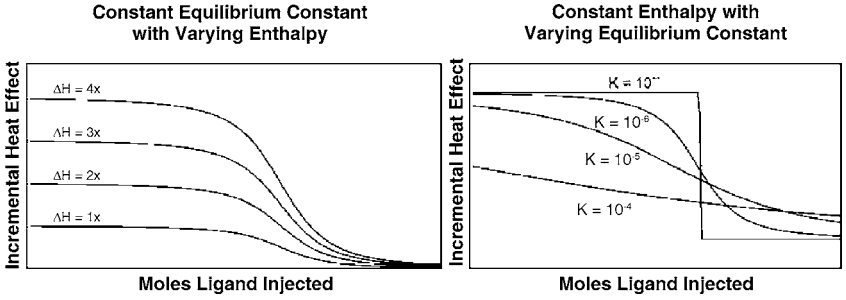

Fig. 9. The effects of the magnitudes of ΔH and K on the shape of a calorimetric titration curve for a reaction with 1:1 stoichiometry.

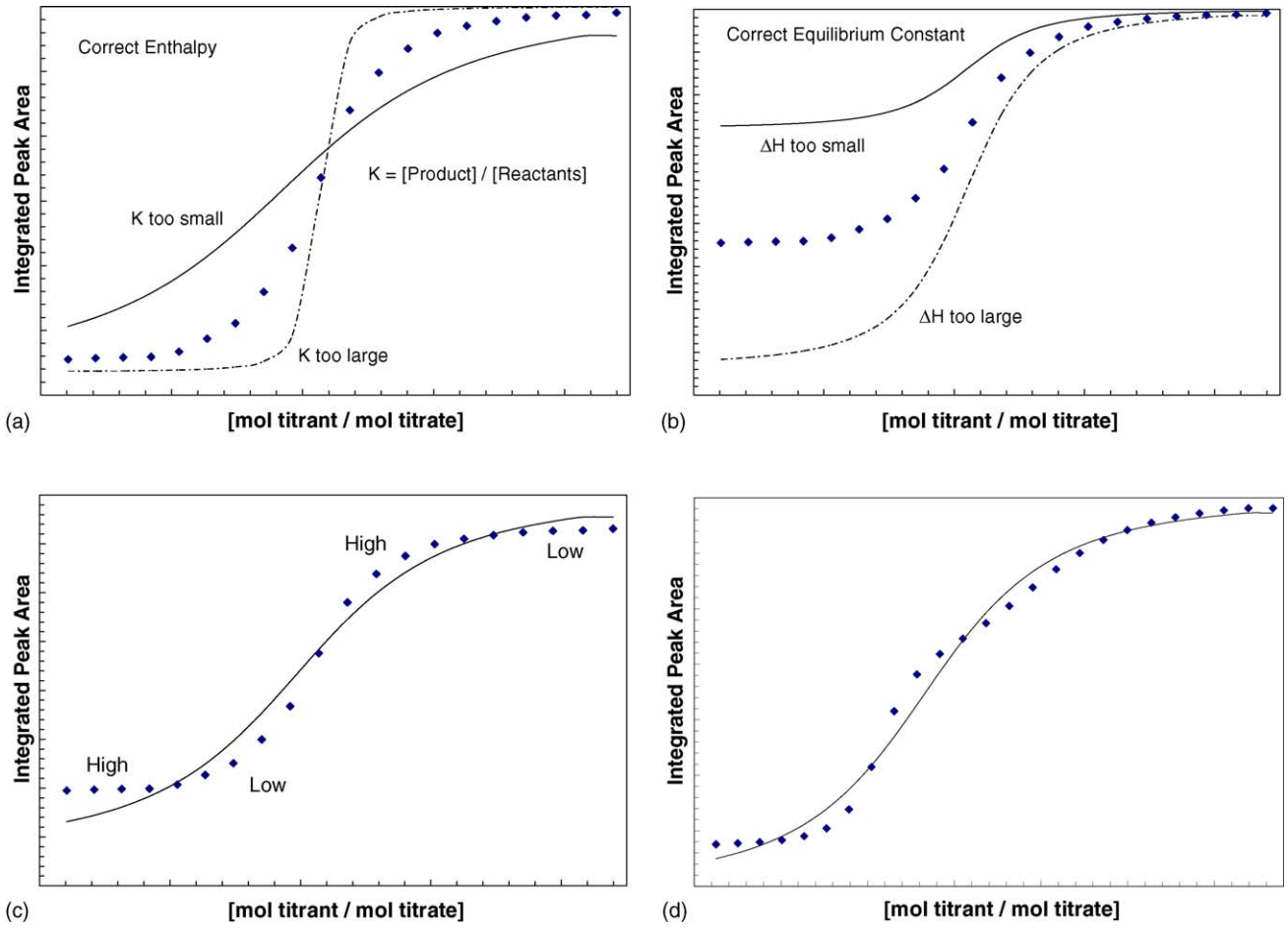

Fig. 10. Effects of errors in fitting models to calorimetric titration curves. Part (a) shows the effects of incorrect K values with a correct ΔH value. Part (b) shows the effects of incorrect ΔH values with a correct K value. Part (c) shows the effect of an incorrect blank or dilution correction, which causes oscillation of residual errors. Part (d) shows the results of fitting a reaction system with two independent sites ($2L + P = PL_2$) with different K values to a model with variable number of sites, but only one K value, again causing oscillation of residual errors.

by practitioners of this method is collecting too few data points in the curved portion around the equivalence point, which leads to inaccurate K values. Fig. 10c illustrates the effects of some procedural errors, such as an incorrect blank or wrong correction for dilution effects. Another common error is assuming that all reactions have 1:1 stoichiometry. Systems with more than one reaction can give titration curves that appear to be fit by the equations for 1:1 stoichiometry, but close examination usually shows systematic errors in the fit to the experimental data, see Fig. 10d. Plots of residuals should always be examined to detect such systematic errors and can be used to guide determination of the actual stoichiometry of the system. The calorimetric method can be expanded to solve for equilibrium constants and enthalpy changes for multiple, simultaneous equilibria (e.g. see [14,20–22].

Equilibrium constants for phase equilibria such as between monomers and micelles or between a solid and a solution can also be determined by titration calorimetry. For example, Fig. 11 shows the determination of the critical micelle concentration (CMC) for a typical amphiphile. The enthalpy change for micelle formation, which is dependent on the medium, is also available from such a titration. Solubilities of moderately insoluble solids can be determined by titration of a saturated solution containing a slight excess of the solid with solvent. Miscibilities of liquids can be determined by titration of one liquid into the other. When the solubility or miscibility limit is reached, the reaction stops and no further heat is produced.

The great advantage of heat conduction or power-compensation calorimetry for measuring kinetics of very slow reactions is that rates are measured directly [11]. Such a measurement takes much less calendar time than measuring the change in the amount of reactants or products after a period of time. For this reason, calorimetry has become widely used for determination at ambient temperature of the kinetics of very slow reactions such as hydrolysis of organic compounds and oxidation and crystallization reactions. Fig. 12 shows a sample set of data collected on hydrolysis of aspirin.

Data for reactions with only one reactant can be analyzed by Eq. (9) [41–48]

$$\frac{\mathrm{d}Q}{\mathrm{d}t} = k\,\Delta H\left[A - \left(\frac{Q}{\Delta H}\right)\right]^n \tag{9}$$

where k is the rate constant, A the initial amount of reactant, and n is the order of the reaction. For a first order reaction, the

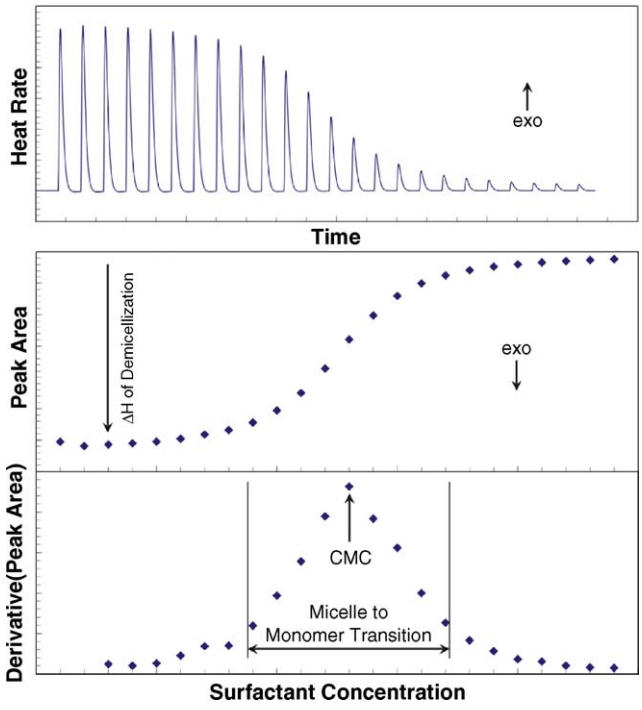

Fig. 11. Determination of critical micelle concentration (CMC) and enthalpy change for the reaction, micelle → monomers, in a CSC model 4500 INC titration cell.

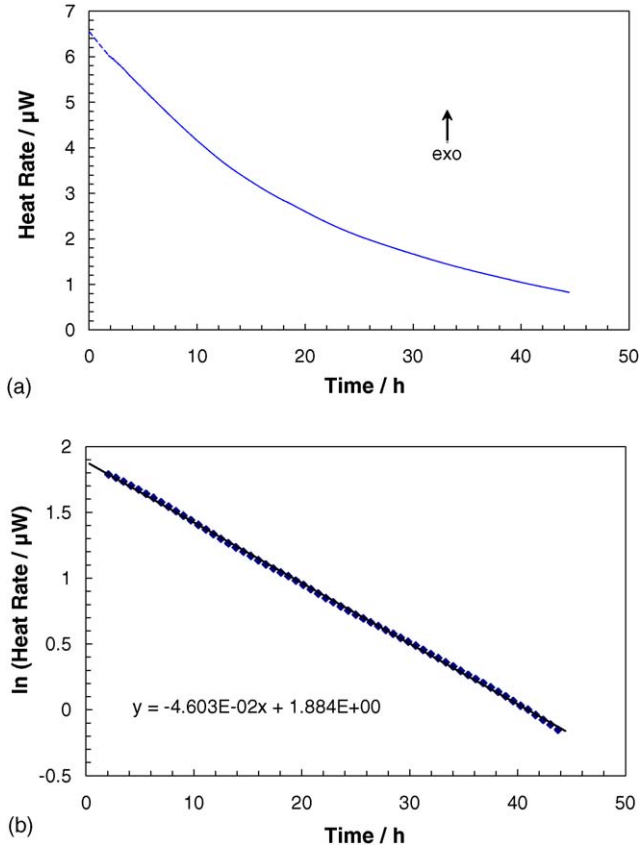

Fig. 12. Baseline corrected raw data for hydrolysis of aspirin (1 mL of 5 mg mL^{-1} in pH 7 phosphate buffer) in a CSC model 5300 ITC-III are shown in part (a). Part (b) shows a log–linear plot of the data demonstrating the reaction is first order in aspirin concentration and giving $k = 4.6 \times 10^{-2}$ h^{-1} and $\Delta H = -18.5$ kJ mol^{-1}.

Table 2
Ratios of times at which the reaction reaches the percent completions for differing reaction orders

Reaction order	Calculated constant ($t_{10\%}/t_{99\%}$)	Calculated constant ($t_{10\%}/t_{90\%}$)	Calculated constant ($t_{25\%}/t_{99\%}$)	Calculated constant ($t_{25\%}/t_{90\%}$)
0.1	16.04	2.264	11.55	1.631
0.3	42.93	4.564	41.44	4.405
0.5	89.96	8.996	74.96	7.496
0.7	145.8	14.20	104.1	10.14
0.9	202.2	19.39	127.8	12.26
1.1	254.6	24.18	146.8	13.94
1.3	301.9	28.48	162.3	15.31
1.5	343.9	32.29	175.0	16.43
1.7	381.0	35.63	185.5	17.35
1.9	414.1	38.61	194.5	18.13
2.1	443.0	41.23	202.0	18.80
2.3	469.6	43.57	208.8	19.38
2.5	493.0	45.67	214.5	19.87
2.7	513.5	47.53	219.4	20.31
2.9	532.9	49.21	224.1	20.69

integral form of Eq. (9) is

$$-\ln\left[A - \left(\frac{Q}{\Delta H}\right)\right] = kt \tag{10}$$

Substitution of Eq. (9) into Eq. (10) to eliminate $[A - (Q/\Delta H)]$ then gives

$$\ln\left(\frac{\mathrm{d}Q}{\mathrm{d}t}\right) = \ln(k\,\Delta H) - kt \tag{11}$$

which shows that a plot of ln(heat rate) versus time is linear with a slope equal to $-k$ for a first order reaction. That this is the case for hydrolysis of aspirin is shown by the plot in Fig. 12b. Once k is known, ΔH can be estimated from the intercept of the plot. This approach can be expanded to include any type of rate law [41–48].

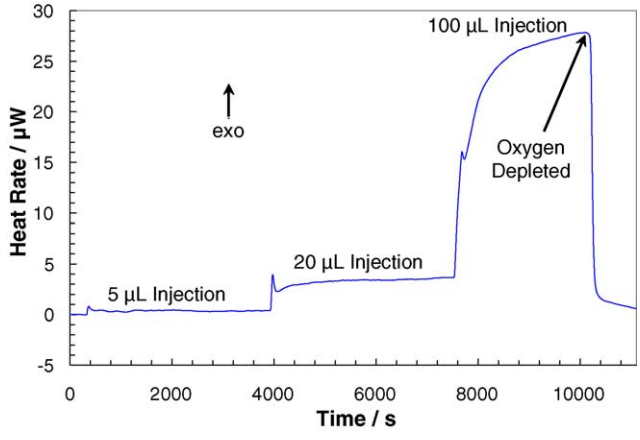

Fig. 13. Baseline corrected data for three different concentrations of *Micrococcus lysodeikticus* culture diluted into water in a CSC model 5300 ITC-III. The heat rates are approximately proportional to cell concentration. The slopes of the lines (at 2000–4000 s, 6.69×10^{-5} μW s^{-1}; at 5600–7400 s, 2.59×10^{-4} μW s^{-1}; and at 9000–10000 s, 1.36×10^{-3} μW s^{-1}) are directly proportional to the number of cells, and thus, proportional to the growth rate. Oxygen in the medium was depleted at about 10,000 s.

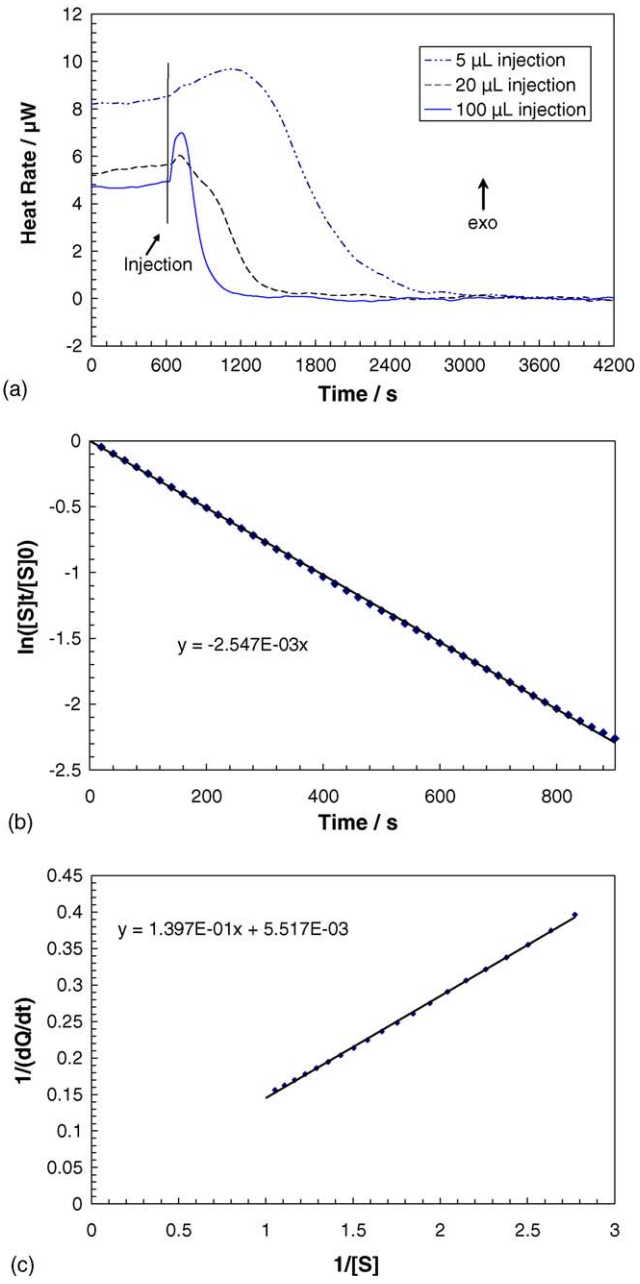

Fig. 14. Part (a) shows batch injections of 0.1 mg mL^{-1} lysozyme into *Micrococcus lysodeikticus* culture in a CSC model 5300 ITC-III. Part (b) shows a log–linear plot of the data in part a from the curve for the 5 μL injection from 1600 to 2500 s. $[S]/[S]_0$ is the ratio of the heat rates where $[S]_0$ is the heat rate at 1600 s, i.e. time zero. Part (c) shows a Lineweaver–Burk double reciprocal plot of the same data.

For reactions described by Eq. (9), the ratio of the times at which the ratio of the rates reaches a particular value is a function only of n [41–48]. For example, for a first order reaction, the ratio of the times at which the rates are $dQ/dt = 0.25(dQ/dt)_{t=0}$ and $dQ/dt = 0.90(dQ/dt)_{t=0}$ is equal to 13.1. For the data in Fig. 12 $(dQ/dt)_{t=0} = 6.56$ μW, and the times at which $dQ/dt = 90$ and 25% of this value are, respectively, 2.28 and 30.2 h which gives a ratio of 13.2. Table 2 gives values of the time ratios for various reaction orders and four different pairs of fractions of the initial rate.

Metabolic rates of living organisms are also of particular interest in biotechnology (e.g. see [1,4,5]. Fig. 13 shows the heat rates produced by addition of a fresh culture of *Micrococcus lysodeikticus* to water. The heat rates are proportional to the concentration or number of live cells in the calorimeter. The change in the heat rate with time (i.e. $d(dQ/dt)/dt$) after an injection is also proportional to the number of cells injected, and is apparently due to growth of the organism, that is, the slope of the line is proportional to the growth rate.

Fig. 14 shows how one can take advantage of the easily measured metabolic heat rate to measure the toxicity and kinetics of killing of an organism by a very dilute solution of a toxin (for other examples, see [1,5,7]). In the example shown in Fig. 14a, lysozyme lysis the cells by punching holes in the cell membrane. Two effects are present in the curves shown, growth causes an increase in the metabolic heat rate as seen in the early part of the curves, and lysis causes the heat rate to decrease during the latter part of the curve. This latter part can be analyzed with Michaelis–Menten kinetics [49,50] as shown in Fig. 14b where $[S]_t/[S]_0$ is simply equal to the ratio of the heat rates at time = t and time = 0 as required by first order kinetics. The data can also be plotted as a Lineweaver–Burk double reciprocal plot as shown in Fig. 14c. In this example, the heat rate actually measures the substrate concentration, i.e. the number of live cells in the solution.

Acknowledgements

The authors thank David Thomas for assistance in collecting much of the data given in the paper. Financial support from CSC and BYU is appreciated.

References

[1] R.B. Kemp (Ed.), Handbook of Thermal Analysis and Calorimetry: From Macromolecules to Man, vol. 4, Elsevier Science, Amsterdam, 1999.
[2] S.E. Harding, B.Z. Chowdhry, Protein-Ligand Interactions: Hydrodynamics and Calorimetry, Oxford University Press, Oxford, 2001.
[3] P.J. Haines (Ed.), Principles of Thermal Analysis and Calorimetry, The Royal Society of Chemistry, Cambridge, 2002.
[4] L.D. Hansen, C. Macfarlane, N. McKinnon, B.N. Smith, R.S. Criddle, Thermochim. Acta 422 (2004) 55–61.
[5] D. Lörinczy (Ed.), The Nature of Biological Systems as Revealed by Thermal Methods, Kluwer Academic, Dordrecht, 2004.
[6] G. Buckton, S.J. Russell, A.E. Beezer, Thermochim. Acta 193 (1991) 195–214.
[7] A.E. Beezer (Ed.), Biological Microcalorimetry, Academic Press, New York, 1980.
[8] G. Buckton, A.E. Beezer, Int. J. Pharm. 72 (1991) 181–191.
[9] L.D. Hansen, Pharm. Tech. 20 (1996) 64–74.
[10] L.D. Hansen, Ind. Eng. Chem. Res. 39 (2000) 3541–3549.
[11] L.D. Hansen, E.A. Lewis, D.J. Eatough, R.G. Bergstrom, D. DeGraft-Johnson, Pharm. Res. 6 (1988) 20–27.
[12] L.D. Hansen, D.J. Eatough, E.A. Lewis, Can. J. Chem. 68 (1990) 2111–2114.
[13] A.J. Fontana, L. Howard, R.S. Criddle, L.D. Hansen, E. Wilhelmsen, J. Food Sci. 58 (1993) 1411–1417.
[14] D.J. Eatough, E.A. Lewis, L.D. Hansen, in: K. Grime (Ed.), Analytical Solution Calorimetry, John Wiley & Sons, New York, 1985, pp. 137–161.

[15] T. Wiseman, S. Williston, J. Brandts, L.N. Lin, Anal. Biochem. 179 (1989) 131–137.
[16] L.D. Hansen, E.A. Lewis, D.J. Eatough, in: K. Grime (Ed.), Analytical Solution Calorimetry, John Wiley & Sons, New York, 1985, pp. 57–95.
[17] L.D. Hansen, Thermochim. Acta 371 (2001) 19–22.
[18] J.J. Christensen, R.M. Izatt, L.D. Hansen, Rev. Sci. Instrum. 36 (1965) 779–783.
[19] L.D. Hansen, D.J. Eatough, Thermochim. Acta 70 (1983) 257–268.
[20] J.J. Christensen, J. Ruckman, D.J. Eatough, R.M. Izatt, Thermochim. Acta 3 (1972) 203–218.
[21] D.J. Eatough, J.J. Christensen, R.M. Izatt, Thermochim. Acta 3 (1972) 219–232.
[22] D.J. Eatough, R.M. Izatt, J.J. Christensen, Thermochim. Acta 3 (1972) 233–246.
[23] N. Markova, D. Hallén, Analyt. Biochem. 331 (2004) 77–88.
[24] M.J. Larsen, D.J.B. Hemming, R.G. Bergstrom, R.W. Wood, L.D. Hansen, Int. J. Pharm. 154 (1997) 103–107.
[25] R.S. Criddle, R.W. Breidenbach, A.J. Fontana, L.D. Hansen, Thermochim. Acta 216 (1993) 147–155.
[26] L.D. Hansen, J.W. Crawford, D.R. Keiser, R.W. Wood, Int. J. Pharm. 135 (1996) 31–42.
[27] L.D. Hansen, M.T. Pyne, R.W. Wood, Int. J. Pharm. 137 (1996) 1–9.
[28] S.L. Randzio, D.J. Eatough, E.A. Lewis, L.D. Hansen, J. Chem. Thermodynamics 20 (1988) 937–948.
[29] G. Defossemont, S.L. Randzio, B. Legendre, Cryst. Growth Des. 4 (2004) 1169–1174.
[30] S.L. Randzio, Thermochim. Acta 398 (2003) 75–80.
[31] S.L. Randzio, Thermochim. Acta 355 (2000) 107–113.
[32] S.L. Randzio, J. Thermal Analyt. 48 (1997) 573–583.
[33] S.L. Randzio, Chem. Soc. Rev. 25 (1996) 383.
[34] J.F. Brandts, L.N. Lin, Thermochim. Acta 414 (2004) 95–100.
[35] H. Heerklotz, J. Physics, Condens. Matter 16 (2004) R441–R467.
[36] J.R. Lepock, Methods 35 (2005) 117–125.
[37] L.D. Hansen, J.J. Christensen, R.M. Izatt, J. Chem. Soc, Chem. Commun. 3 (1965) 36–37.
[38] J.J. Christensen, R.M. Izatt, L.D. Hansen, J.A. Partridge, J. Phys. Chem. 70 (1966) 2003–2010.
[39] J.M. Sturtevant, in: H.A. Skinner (Ed.), Experimental Thermochemistry, vol. II, Interscience, NY, 1962, pp. 427–442.
[40] A.A. Saboury, J. Thermal Anal. Cal. 72 (2003) 93–103.
[41] A.E. Beezer, S. Gaisford, A.K. Hills, R.J. Willson, J.C. Mitchell, Int. J. Pharm. 179 (1999) 159–165.
[42] A.E. Beezer, R.J. Willson, J.C. Mitchell, A.K. Hills, S. Gaisford, E. Wood, J.A. Connor, Pure Appl. Chem. 70 (1998) 633–638.
[43] S. Gaisford, A.K. Hills, A.E. Beezer, J.C. Mitchell, Thermochim. Acta 328 (1999) 39–45.
[44] A.E. Beezer, Thermochim. Acta 380 (2001) 205–208.
[45] A.E. Beezer, A.C. Morris, M.A.A. O'Neill, R.J. Willson, A.K. Hills, J.C. Mitchell, J.A. Connor, J. Phys. Chem. B 105 (2001) 1212–1215.
[46] M.A.A. O'Neill, A.E. Beezer, A.C. Morris, K. Urakami, R.J. Willson, J.A. Connor, J. Thermal Anal. Cal. 73 (2003) 709–714.
[47] R.J. Willson, A.E. Beezer, Thermochim. Acta 402 (2003) 75–80.
[48] A.E. Beezer, M.A.A. O'Neill, K. Urakami, J.A. Connor, J. Tetteh, Thermochim. Acta 417 (2004) 19–22.
[49] M.A.A. O'Neill, A.E. Beezer, J.C. Mitchell, J. Orchard, J.A. Connor, Thermochim. Acta 417 (2004) 187–192.
[50] M.J. Todd, J. Gomez, Analyt. Biochem. 296 (2001) 179–187.